



Reduced immunoreactivities of B-type natriuretic peptide in pulmonary arterial hypertension rats after ranolazine treatment

Jae Chul Lee^{1,2,3,4}, Kwan Chang Kim⁵, Soo Young Choe¹, Young Mi Hong⁴

¹Department of Biology, School of Life Sciences, Chungbuk National University, Cheongju, ²Department of Surgery, Brain Korea 21 PLUS Project for Medical Sciences and HBP Surgery and Liver Transplantation, Korea University College of Medicine, Seoul, ³Department of Anatomy, Seoul National University College of Medicine, Seoul, Departments of ⁴Pediatrics and ⁵Thoracic and Cardiovascular Surgery, Ewha Womans University School of Medicine, Seoul, Korea

Abstract: Pulmonary arterial hypertension (PAH) is a severe pulmonary vascular disease characterized by sustained increase in the pulmonary arterial pressure and excessive thickening and remodeling of the distal small pulmonary arteries. During disease progression, structural remodeling of the right ventricular (RV) impairs pump function, creates pro-arrhythmic substrates and triggers for arrhythmias. Notably, RV failure and lethal arrhythmias are major contributors to cardiac death in PAH that are not directly addressed by currently available therapies. Ranolazine (RAN) is an anti-anginal, anti-ischemic drug that has cardioprotective effects of heart dysfunction. RAN also has anti-arrhythmic effects due to inhibition of the late sodium current in cardiomyocytes. Therefore, we hypothesized that RAN could reduce the mal-adaptive structural remodeling of the RV, and prevent triggered ventricular arrhythmias in the monocrotaline-induced rat model of PAH. RAN reduced ventricular hypertrophy, reduced levels of B-type natriuretic peptide, and decreased the expression of fibrosis. In addition, RAN prevented cardiovascular death in rat model of PAH. These results support the notion that RAN can improve the functional properties of the RV, highlighting its potential benefits in the setting of heart impairment.

Key words: B-type natriuretic peptide, Heart, Pulmonary artery hypertension, Ranolazine, Right ventricles

Received August 19, 2015; Revised January 25, 2016; Accepted March 7, 2016

Introduction

Pulmonary arterial hypertension (PAH) is a disease characterized by vascular remodeling and vasoconstriction of the pulmonary arterial circulation that results in right

ventricular (RV) failure. The progressive vasculopathy leads to intraluminal narrowing and obstruction of the resistance vasculature leading to sustained increases in pulmonary vascular resistance [1]. Nevertheless, most common and aggressive form results from wall thickening in small pulmonary arteries, of uncertain aetiology, but often observed in association with systemic diseases. A widely accepted experimental model of PAH is generated by systemic administration of monocrotaline (MCT), a vascular toxin that selectively affects the pulmonary microcirculation [2]. PAH imposes a high pressure load on the RV and leads to progressive remodelling. Albeit initially compensatory, the process becomes mal-adaptive, thus making the development of RV dysfunction the turning point in PAH prognosis [3]. Despite some clinical successes with therapies, PAH remains

Corresponding authors:

Soo Young Choe

Department of Biology, School of Life Sciences, Chungbuk National University, 1 Chungdae-ro, Seowon-gu, Cheongju 28644, Korea
Tel: +82-43-261-2297, Fax: +82-43-275-2291, E-mail: leejc@chungbuk.ac.kr
Young Mi Hong

Department of Pediatrics, Ewha Womans University School of Medicine, 1071 Anyangcheon-ro, Yangcheon-gu, Seoul 07985, Korea
Tel: +82-2-2286-1431, Fax: +82-2-2286-1432, E-mail: beas100@snu.ac.kr

Copyright © 2016. Anatomy & Cell Biology

This is an Open Access article distributed under the terms of the Creative Commons Attribution Non-Commercial License (<http://creativecommons.org/licenses/by-nc/4.0/>) which permits unrestricted non-commercial use, distribution, and reproduction in any medium, provided the original work is properly cited.

a severe disease [4]. Thus, new therapies for PAH should protect against RV maladaptation and failure [5].

Plasma B-type natriuretic peptide (BNP) and its N-terminal pro-form, NT-proBNP, are increased in many cardiac entities and predict poor prognosis in systolic and diastolic heart failure, and pulmonary embolism. Natriuretic peptides, especially BNP, also aid in evaluating symptoms of congestive heart failure and in discriminating between cardiac and noncardiac dyspnea [6, 7]. BNP is a “true” cardiac hormone released from atrial and ventricular myocardium in response to intracardiac pressure increases [8]. The secreted pre-pro-form is cleaved into the N-terminal pro-peptide with a longer half-life and the mature form BNP; both can be accurately measured in the plasma. Because of a longer half-life, plasma levels of NT-proBNP are 5- to 10-fold greater than BNP. Diastolic stretch induces myocardial BNP expression in the myocyte in volume-overload states like congestive heart failure, severe aortic regurgitation [9]. Pressure overload as in severe aortic stenosis also increases wall stress and myocardial release of BNP [6].

Previous investigations have established a role for BNP as a biomarker for diagnosis and prognostication, management of patients with heart failure and pulmonary hypertension [6, 10]. Ranolazine (RAN), is a Food and Drug Administration (FDA)-approved anti-anginal drug with anti-ischemic activity that has also been shown to have anti-arrhythmic properties due to inhibition of the late sodium current (I_{Na}) in cardiomyocytes [11, 12]. As a result of extensive clinical and experimental studies, the cardioprotective effects of RAN in settings of left-sided heart dysfunction are well established [13-15]. Although the left ventricle (LV) and RV have notable and well-defined differences, common mechanisms such as ischemia, Ca^{2+} overload, oxidative stress, and fibrosis are implicated in the pathology of both left- and right-sided heart failure [16-19]. It has also been reported that RAN can reduce RV hypertrophy in a rat model where RV pressure-overload is induced independently from changes in pulmonary arterial pressures by pulmonary artery banding [20]. Additionally, a recent study in 21 days MCT rat model showed that RAN, when initiated 2 days after MCT injection, prevented RV structural and electrical remodeling by suppressing late I_{Na} [21]. In our study, RAN treatment was started at 7 days following MCT injection to allow for the vasculopathy to develop prior to intervention, and all endpoints were assessed 28 days following MCT. We using an immunohistochemical approach, reverse transcription-polymerase chain reaction

(RT-PCR) and western blotting of *in vivo* approaches to determine the changes of BNP immunoreactivity if RAN treatment could reduce the development of the PAH in a model.

Materials and Methods

Animals

Six-week-old male Sprague-Dawley rats were used. All rats were housed in climate-controlled conditions with a 12-hour light/12-hour dark cycle, and had free access to food and water. All animal experiments were approved by the appropriate Institutional Review Boards of the Seoul National University College of Medicine (Seoul, Korea; SNU-141202-2) and conducted in accordance with National Institutes of Health Guide for the Care Use of Laboratory Animals (NIH publication No. 86-23, revised in 1996).

PAH rat model

PAH was induced by subcutaneous injection of 50 mg/kg MCT (Sigma-Aldrich, St. Louis, MO, USA) dissolved in 0.5 N HCl. All animals had free access to standard rodent chow and water for the first week post-MCT injection, thereafter subsets of rats were switched to a diet containing 0.5% RAN by weight to determine the effect of chronic RAN administration during PAH development. The rats were grouped as follows: control group (C group, n=20), vehicle injection and normal diet; monocrotaline group (M group, n=20), MCT injection and normal diet; Ranolazine group (RAN group, n=20), MCT injection and diet containing 0.5% RAN. The animals were sacrificed at 7, 14, 21, and 28 days (each group, n=5) after RAN administration. Tissues were removed and immediately frozen at -70°C for enzyme analysis.

Determination of the organ weights and right hypertrophy index

The rats were weighed and observed for general appearance during the study period. The animals were sacrificed at the scheduled time. The wet weights of excised RV, LV plus interventricular septum (IVS) (LV+IVS) were measured. The RV to LV+IVS ratio [RV/(LV+IVS)] was used to determine the right hypertrophy index (RVI). The standard of RV hypertrophy was defined as an RVI >0.33 [22].

Pulmonary haemodynamics

Rats were anaesthetized by intraperitoneal injection of

urethane and secured on a surgical stage. An 8-mm-long right internal jugular vein was isolated and ligated at the distal end. The vessel was cut at the proximal end of ligation. A catheter filled with heparin saline was rapidly inserted along the incision and slowly advanced for about 5 cm to enter the pulmonary artery. The standard of pulmonary hypertension was defined as systolic pulmonary artery pressure (SPAP) >50 mm Hg [23]. Hemodynamic parameters were recorded at baseline and at 7, 14, 21, and 28 days.

Histologic findings of pulmonary arteries

Heart and lung tissues were fixed with 10% buffered formalin and then embedded in paraffin. Sections were performed by 4- μ m-thick hematoxylin and eosin (H&E) stains to evaluate histopathologic changes of pulmonary blood vessels. The small pulmonary artery wall thickness (SPAWT) was expressed as follows: % wall thickness.

Masson trichrome staining

Masson trichrome staining was carried out in accordance with well-characterized protocols. Briefly, heart tissue sections were deparaffinized and hydrated in distilled water prior to a 1-hour treatment in Bouin's fixative (catalog #NC9674780, Richard-Allan Scientific, Kalamazoo, MI, USA) at 56°C. Sections were washed in running distilled water until clear, and then stained in Weigert's iron hematoxylin (catalog #NC9231529, Richard-Allan Scientific) for 10 minutes. Following a 10-minute wash in running water, sections were stained in Biebrich scarlet-acid fuchsin (catalog #NC9424144, Richard-Allan Scientific) for 2 minutes. Sections were rinsed in distilled water followed by a 10-minute differentiation in phosphomolybdic-phosphotungstic acid (catalog #NC9443038, Richard-Allan Scientific). Aniline blue (catalog #NC9684104, Richard-Allan Scientific) was used as a counterstain for 10 minutes, and then sections were differentiated in 1% acetic acid for 3 minutes. Sections were dehydrated through a series of graded alcohols back to xylene, and then coverslipped and sealed using Cytoseal XYL (Richard-Allan Scientific).

Masson's trichrome staining image analysis

Masson's trichrome staining was performed. It is used in order to observe the degree of collagen fiber penetrating using light microscopy. The photographs were processed through an image analysis program (anaylySIS) and the degree of collagen fiber was measured by image j (National Institutes of Health, Bethesda, MD, USA). To verify the differences within

each group, we implemented Duncan's multiple range test.

BNP mRNA expression studies

Total RNA was isolated from heart tissue samples of C group, M group, and RAN group rats at 28 days using TRI reagent (Invitrogen, Carlsbad, CA, USA), according to the manufacturer's guidelines. The resulting total RNA was subjected to DNase treatment using RNase-free DNase (Ambion, Austin, TX, USA). The purity of isolated RNA was measured by a NanoDrop spectrophotometer (Thermo Fisher Scientific, Wilmington, USA). A set concentration of RNA was reverse transcribed into cDNA, and semi-quantitative polymerase chain reaction (PCR) was performed on Gene Amp PCR system 9600 (Applied Biosystems, Foster City, CA, USA). The primer and probe sequences are shown below. BNP: sense 5'-CATCACTTCTGCAGCATGG-3', anti-sense 5'-GCCGGAGTCTGCAGCCAGG-3'; glyceraldehyde 3-phosphate dehydrogenase: sense 5'-GCACAGTCAAGGCCGAGAAT-3', antisense 5'-GCC TTCTCCATGGTGGTGAA-3'. An AccuPower DualStar PCR PreMix kit (Bioneer, Daejeon, Korea) was used for 20 μ l reactions. The 20 μ l of synthesized cDNA reactant was diluted in 80 μ l of DEPC-treated distilled water, and 3 μ l of the solution was used as a PCR template. The reaction medium composition was as follows: PCR forward primer, 10 pmol, 1 μ l; PCR reward primer, 10 pmol, 1 μ l; Taqman probe, 10 pmol, 1 μ l; template, 3 μ l; DEPC-treated distilled water, 14 μ l. All primers were amplified using the same conditions. Thermal cycling conditions 50°C for 2 minutes and 95°C for 10 minutes followed by 40 cycles of 95°C for 30 seconds and 60°C for 30 seconds, 72°C for 30 seconds. PCR product was run in a 1% agarose gel and visualized under UV light.

Western blot analysis

The tissue was homogenized in 10 mM Tris-HCl buffer, pH 7.4 containing 0.5 mM EDTA, pH 8.0, 0.25 M sucrose, 1 mM phenylmethylsulfonyl fluoride, 1 mM Na₄VO₃, and a protease inhibitor cocktail (Roche-Boehringer-Mannheim, Mannheim, Germany). After centrifugation, the supernatant was subjected to sodium dodecyl sulfate polyacrylamide gel electrophoresis (SDS-PAGE). Samples equivalent to 25 μ g of protein content were loaded and size-separated in 8%–12% SDS-PAGE. The proteins on the acrylamide gel were transferred to a polyvinylidene difluoride membrane (Millipore, Bedford MA, USA) at 400 mA in a transfer buffer containing 25 mM Tris and 192 mM glycine, pH 8.4. The

nitrocellulose membranes was blocked in tris-buffered saline with 5% non-fat dry milk at room temperature for 1 hour in 0.1% Tween 20 and incubated with the appropriated primary antibodies, including anti-BNP (Santa Cruz Biotechnology Inc., Santa Cruz, CA, USA) and anti-actin (Santa Cruz Biotechnology Inc.), at 4°C overnight. The membranes were then incubated with horseradish peroxidase-conjugated secondary antibody (Cell Signaling Technology Inc., Danvers, MA, USA) for 1 hour at room temperature. After washing, the membranes were visualized by a chemiluminescent ECL-detection kit from GE-Healthcare (Piscataway, NJ, USA).

Statistical analyses

Results were expressed as the mean±standard deviation. An unpaired two-tailed t test and Mann-Whitney test were used, and a P-value of <0.05 was considered statistically significant. SPSS version 14.0 (SPSS Inc., Chicago, IL, USA) was used for all statistical analyses.

Results

Organ weight

M group showed the increase of RV weight at 21 and 28 days. The weight of LV+IVS was no significant differences between the C, M, and the RAN groups. RV/LV+IVS ratio was significantly increased at 14, 21, and 28 days in the M group compared with the C group. However, RV/LV+IVS ratio was significantly decreased at 28 days in the M group compared with the RAN group. The weight of LV+IVS was significantly lower in the M group and the RAN group compared with the C group at 14, 21, and 28 days. The heart

weight was significantly increased in the M group compared with the C group at 21 and 28 days. However, the heart weight was significantly decreased in the RAN group compared with the M group at 28 days (Table 1).

Changes in SPAP after RAN treatment in PAH rats

The mean SPAP was significantly increased in the M group compared with the C group at 14, 21, and 28 days. SPAP was significantly decreased in the RAN group compared with the M group at 21 and 28 days (Table 1).

Changes in structural remodeling after RAN treatment in PAH rats

To provide preliminary information on the mechanism

Table 1. Changes of SPAP and organ weights after RAN treatment in PAH rats

Day	Group	SPAP (mm Hg)	RV (g)	LV+IVS (g)	RV/(LV+IVS) (%)
7	Control	22.1±1.3	0.141±0.03	0.552±0.03	0.25±0.19
	M	30.4±2.5	0.151±0.02	0.539±0.02	0.28±0.21
	RAN	30.1±2.7	0.154±0.03	0.548±0.03	0.28±0.18
14	Control	21.4±1.1	0.150±0.03	0.682±0.03	0.21±0.20
	M	38.4±3.2*	0.212±0.06	0.656±0.05	0.32±0.32*
	RAN	32.4±2.4	0.164±0.05	0.689±0.04	0.23±0.25
21	Control	22.8±1.4	0.166±0.03	0.751±0.04	0.21±0.23
	M	50.4±6.3*	0.299±0.05*	0.653±0.04	0.45±0.54*
	RAN	44.2±4.3 [#]	0.184±0.07	0.698±0.05	0.26±0.42
28	Control	22.4±1.0	0.170±0.04	0.789±0.04	0.21±0.25
	M	65.2±9.3*	0.354±0.09*	0.721±0.07	0.49±0.64*
	RAN	45.3±3.6 [#]	0.201±0.11 [#]	0.742±0.05	0.27±0.35 [#]

Values are presented as mean±standard deviation. SPAP, systolic pulmonary artery pressure; RAN, 0.5% ranolazine; PAH, pulmonary arterial hypertension; RV, right ventricle; LV, left ventricle; IVS, interventricular septum; M, monocrotaline. *P<0.05 compared with the C group, [#]P<0.05 compared with the M group.

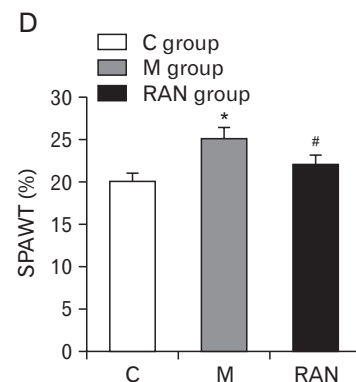
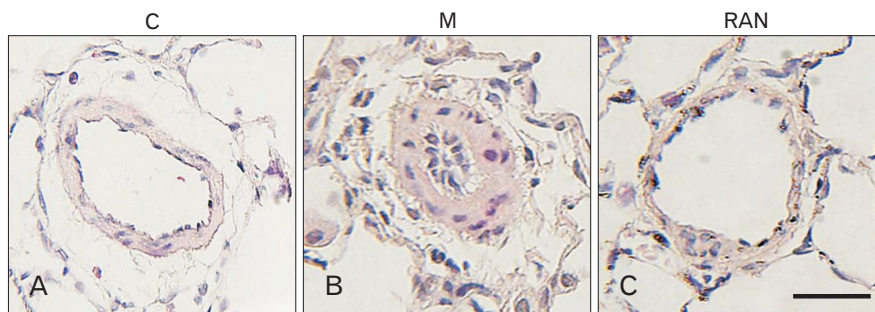


Fig. 1. Pulmonary vascular remodeling. Examples of hematoxylin and eosin stained lung sections (A, C group; B, M group; C, RAN group) and statistics for small pulmonary artery wall thickness (SPAPWT) measurements (D). C group, control group; M group, monocrotaline group; RAN group, ranolazine group. n=10 for each group. *P<0.05 vs. C group, [#]P<0.05 vs. M group. Scale bars=50 µm.

accounting for RAN prevention of MCT-induced increment in RV systolic pressure, SPAWT was measured. As shown in Fig. 1, relative medial SPAWT was increased in the MCT group (+20%), a change prevented by RAN ($P=0.0033$ vs. C group, $P=0.0192$ vs. M group).

Administration of RAN reduces RV collagen deposition

To evaluate the effect of RAN treatment on the development of cardiac fibrosis and remodeling, RV samples were collected 28 days following the injection of MCT for histology patterns in the RV (Fig. 2). RV sections stained with Masson's trichrome showed more pronounced collagen deposition from animals with PAH compared to control and to animals treated with 0.5% RAN ($P=0.001$ vs. C group, $P=0.008$ vs. M group) (Fig. 2).

RT-PCR

BNP mRNA was expressed in the RV of control group. RV from rats with MCT-induced PAH had increased expression of the mRNA transcripts for BNP (Fig. 3). However, the decreased expression of BNP mRNA were significantly decreased in the RAN group compared with the M group ($P=0.006$ vs. C group, $P=0.001$ vs. M group) (Fig. 3).

Western blotting analysis

This experiment was designed to investigate if RAN group exhibited alterations in the levels of expression of the BNP protein in the RV of heart. Changes in the levels of BNP

immunoreactivity in the RV were detected in RAN group. The results showed that the levels of immunoreactivity of BNP protein that were detected in RAN group were significantly decreased compared with M group (Fig. 4). The actin

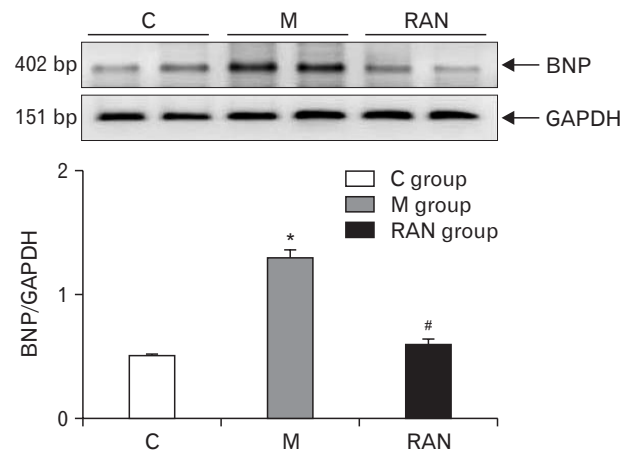


Fig. 3. Expression of B-type natriuretic peptide (BNP) mRNA in the right ventricle. Semi-quantitative reverse transcription polymerase chain reaction (RT-PCR) of BNP is expressed in the control group (C group), monocrotaline group (M group), and ranolazine group (RAN group). No amplification product was found without prior reverse transcription reaction or in water controls (data not shown). RAN group, BNP mRNA is decreased and the pattern of BNP mRNA expression is different. The sizes of RT-PCR products are indicated at left. Band densities were assessed and normalized after standardization of glyceraldehyde 3-phosphate dehydrogenase (GAPDH) band densities to 1. Although samples were screened from five mice in each of the three groups, only a representative single band is shown. * $P<0.05$ vs. C group, # $P<0.05$ vs. M group.

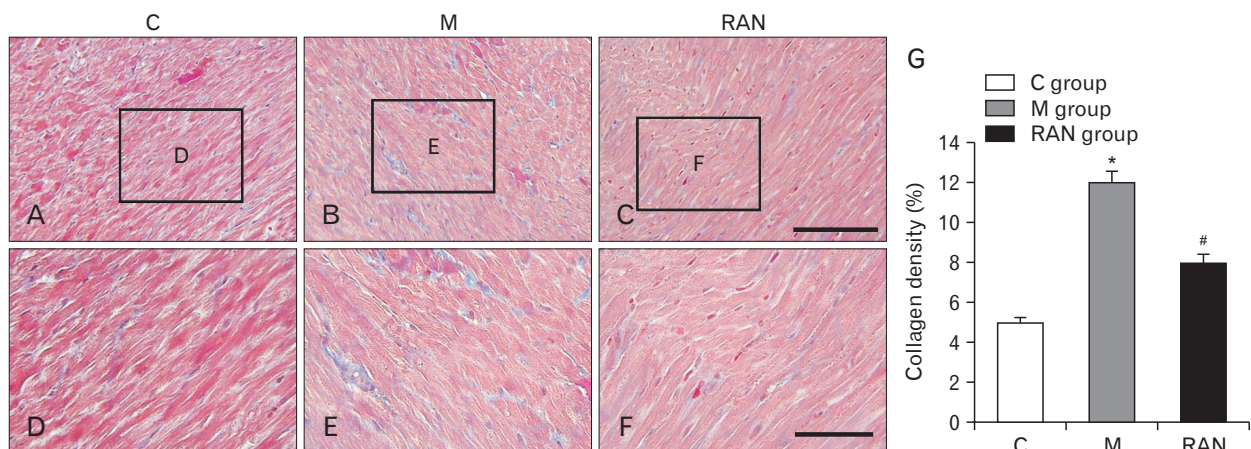


Fig. 2. Representative images of right ventricle (RV) stained with Masson's trichrome from control group (C group) (A), monocrotaline group (M group) (B), and ranolazine group (RAN group) (C) at 28 days following the injection of monocrotaline (MCT). (G) Collagen content was greatly increased in the M group in comparison with the C group at 28 days. The RAN group showed a significant decrease in collagen content at 28 days. Panels (D), (E), and (F) are highpower views of panels (A), (B), and (C); fibrosis is colored blue. * $P<0.05$ vs. C group, # $P<0.05$ vs. M group. $n=10$ for each group. Scale bars=150 μm (A-C), 70 μm (D-F).

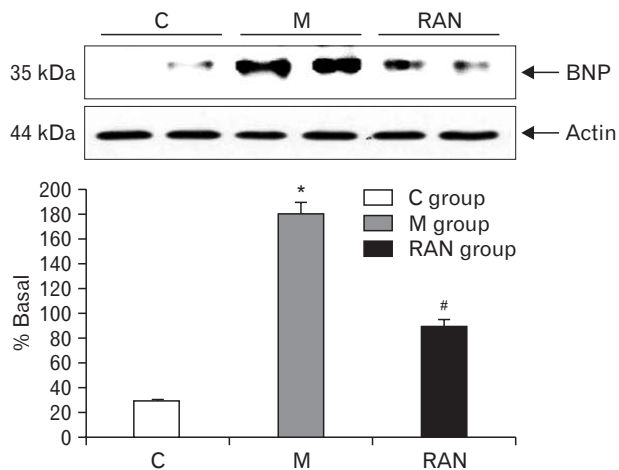


Fig. 4. Western blot analysis of the levels of expression of B-type natriuretic peptide (BNP) and actin immunoreactivity in the right ventricle (RV). The semi-quantitative analysis confirms that ranolazine group (RAN group) exhibited increased levels of immunoreactivity of BNP in the RV (n=4–5 per group). C group, control group; RAN group, ranolazine group. * $P < 0.05$ vs. C group, # $P < 0.05$ vs. M group.

bands indicate protein loading in the same sample ($P < 0.0001$ vs. C group, $P = 0.0004$ vs. M group) (Fig. 4).

Discussion

The present study shows that treatment with RAN reduces mal-adaptive structural remodeling of the RV and prevents triggered ventricular arrhythmias in MCT-induced PAH in rats. Treatment with RAN initiated one week after the injection of MCT led to decreased RV hypertrophy and improved pulmonary hemodynamics. Level of BNP, a clinically validated biomarker of RV failure, were also significantly decreased in rats treated with RAN, indicating improved RV function [24]. In *in vivo* studies using rats with already established PAH and heart remodeling, demonstrated that the acute administration of RAN significantly reduced isoproterenol-induced ventricular tachycardia/ventricular fibrillation and associated cardiovascular death [1]. The results from these *in vivo* experiments support that RAN reduces the arrhythmogenic substrate formation in the heart presumably by decreasing cardiac fibrosis.

The understanding of mal-adaptive RV remodeling was established in experimental studies of left-heart failure. There are prominent embryological and structural differences which preclude the extrapolation of data between the two ventricles [16, 18]. However, many of the same mechanisms have

been described in right-heart failure [17, 18]. In the present study, we used treatment with RAN in PAH rats as an *in vivo* model of PAH and performed H&E staining and Masson's trichrome staining, RT-PCR and western blotting analysis in order to investigate the changes of BNP immunoreactivity in the cardiometer of these rats. A significant increase in pulmonary arterial pressure following MCT injection was accompanied by RV hypertrophy, increased RV fibrosis when compared to control group (Table 1, Fig. 2). In the RV of rats with PAH, RAN treatment decreased the development of ventricular hypertrophy and normalized the expression of collagen content (Fig. 2). Additionally, in hearts from rats with PAH, SPAP of the RV was decreased by RAN treatment. Our results are also consistent with the study conducted by Fang et al. [20] demonstrating that RAN treatment improves RV performance as measured by exercise capacity and cardiac index in rats subjected to RV pressure overload by pulmonary artery banding. BNP, a well-characterized biomarker that is predictive of RV performance, mortality, and clinical outcomes in patients with PAH [24–26]. BNP is produced by and released from ventricular cardiomyocytes and plasma levels of BNP are closely linked to the severity of ventricular remodeling and dysfunction [24, 25, 27]. The effect of RAN to reduce BNP in our study is consistent with the benefits of RAN in animal models of heart disease, and with the amelioration of RV failure in this animal model [3, 13, 28]. Cardiac arrhythmias are major contributors to morbidity and mortality in patients with PAH, can contribute to deteriorations of cardiac function, and are not adequately addressed by current therapies [29, 30]. Importantly, a recent prospective clinical study reported that the restoration of sinus rhythm using antiarrhythmic therapy was associated with a reduction in BNP levels and improved survival [31]. Furthermore, recent studies have shed some light on the therapeutic potential of natriuretic peptides in PAH [32, 33]. The most well-understood physiologic action of BNP is vasodilatation, using cyclic guanosine 3',5'-monophosphate (cGMP) as a second messenger through the binding of membrane bound guanylyl cyclase-A receptor, distinct from the nitric oxide/cGMP pathway that is mediated by the cytosolic guanylyl cyclase [34, 35]. In addition to its vasorelaxant effects, emerging evidence demonstrates that BNP has anti-proliferative effects on human aortic vascular smooth muscle cells, suggesting its potential role in inhibiting vascular remodeling [32, 36]. Indeed, a recent study demonstrates that BNP can attenuate vascular remo-

deling induced by balloon injury rabbit iliac arteries [37]. In addition, we have recently demonstrated that high BNP levels are associated with the patency of ductus arteriosus and poor response to indomethacin, implicating its role in the inhibition of ductus arteriosus closure or remodeling in neonates [38].

The results from studies of RAN treatment in a model of RV dysfunction are also consistent with the well described anti-arrhythmic effects of RAN and action potential duration in order to reduce the arrhythmogenesis of diseased hearts [13, 39]. Rocchetti et al. [21] recently demonstrated that late I_{Na} is enhanced in the RV of MCT rats and blocked by RAN. In addition to inhibiting late I_{Na} , RAN has been reported to inhibit adrenergic receptors and to partially inhibit fatty acid oxidation at high concentrations (>100 μ M) [40]. In the present study RAN, an anti-anginal, anti-ischemic drug known to have beneficial effects in models of LV dysfunction, was efficacious in reducing both structural remodeling of the RV in an animal model of PAH. In conclusion, the chronic administration of RAN during PAH development decreased adverse structural remodeling of the diseased RV, providing evidence that the inhibition of pulmonary artery pressure, RV hypertrophy, RV dysfunction, and the expression of fibrosis content may have beneficial effects in the setting of ventricle impairment due to PAH.

Acknowledgements

The Korea Foundation for the Advancement of Science and Creativity (KOFAC) grant funded by the Korea government (MEST) and supported by a Korea University grant.

References

- Liles JT, Hoyer K, Oliver J, Chi L, Dhalla AK, Belardinelli L. Ranolazine reduces remodeling of the right ventricle and provoked arrhythmias in rats with pulmonary hypertension. *J Pharmacol Exp Ther* 2015;353:480-9.
- Stenmark KR, Meyrick B, Galie N, Mooi WJ, McMurtry IF. Animal models of pulmonary arterial hypertension: the hope for etiological discovery and pharmacological cure. *Am J Physiol Lung Cell Mol Physiol* 2009;297:L1013-32.
- Michelakis ED, Wilkins MR, Rabinovitch M. Emerging concepts and translational priorities in pulmonary arterial hypertension. *Circulation* 2008;118:1486-95.
- Lau EM, Humbert M, Celermajer DS. Early detection of pulmonary arterial hypertension. *Nat Rev Cardiol* 2015;12:143-55.
- Voelkel NF, Bogaard HJ, Gomez-Arroyo J. The need to recognize the pulmonary circulation and the right ventricle as an integrated functional unit: facts and hypotheses (2013 Grover Conference series). *Pulm Circ* 2015;5:81-9.
- Maisel AS, Krishnaswamy P, Nowak RM, McCord J, Hollander JE, Duc P, Omland T, Storrow AB, Abraham WT, Wu AH, Clopton P, Steg PG, Westheim A, Knudsen CW, Perez A, Kazanegra R, Herrmann HC, McCullough PA; Breathing Not Properly Multinational Study Investigators. Rapid measurement of B-type natriuretic peptide in the emergency diagnosis of heart failure. *N Engl J Med* 2002;347:161-7.
- Stanek B, Frey B, Hülsmann M, Berger R, Sturm B, Strametz-Juranek J, Bergler-Klein J, Moser P, Bojic A, Hartter E, Pacher R. Prognostic evaluation of neurohumoral plasma levels before and during beta-blocker therapy in advanced left ventricular dysfunction. *J Am Coll Cardiol* 2001;38:436-42.
- Iwanaga Y, Nishi I, Furuichi S, Noguchi T, Sase K, Kihara Y, Goto Y, Nonogi H. B-type natriuretic peptide strongly reflects diastolic wall stress in patients with chronic heart failure: comparison between systolic and diastolic heart failure. *J Am Coll Cardiol* 2006;47:742-8.
- Vanderheyden M, Goethals M, Verstreken S, De Bruyne B, Muller K, Van Schuerbeeck E, Bartunek J. Wall stress modulates brain natriuretic peptide production in pressure overload cardiomyopathy. *J Am Coll Cardiol* 2004;44:2349-54.
- Rutten FH, Cramer MJ, Zuithoff NP, Lammers JW, Verweij W, Grobbee DE, Hoes AW. Comparison of B-type natriuretic peptide assays for identifying heart failure in stable elderly patients with a clinical diagnosis of chronic obstructive pulmonary disease. *Eur J Heart Fail* 2007;9:651-9.
- Antzelevitch C, Nesterenko V, Shryock JC, Rajamani S, Song Y, Belardinelli L. The role of late I_{Na} in development of cardiac arrhythmias. *Handb Exp Pharmacol* 2014;221:137-68.
- Hale SL, Shryock JC, Belardinelli L, Sweeney M, Kloner RA. Late sodium current inhibition as a new cardioprotective approach. *J Mol Cell Cardiol* 2008;44:954-67.
- Aistrup GL, Gupta DK, Kelly JE, O'Toole MJ, Nahhas A, Chirayil N, Misener S, Beussink L, Singh N, Ng J, Reddy M, Mongkolrattanothai T, El-Bizri N, Rajamani S, Shryock JC, Belardinelli L, Shah SJ, Wasserstrom JA. Inhibition of the late sodium current slows t-tubule disruption during the progression of hypertensive heart disease in the rat. *Am J Physiol Heart Circ Physiol* 2013;305:H1068-79.
- Maier LS, Layug B, Karwadowska-Prokopczuk E, Belardinelli L, Lee S, Sander J, Lang C, Wachter R, Edelmann F, Hasenfuss G, Jacobshagen C. RANoLazIne for the treatment of diastolic heart failure in patients with preserved ejection fraction: the RALI-DHF proof-of-concept study. *JACC Heart Fail* 2013;1:115-22.
- Rastogi S, Sharov VG, Mishra S, Gupta RC, Blackburn B, Belardinelli L, Stanley WC, Sabbah HN. Ranolazine combined with enalapril or metoprolol prevents progressive LV dysfunction and remodeling in dogs with moderate heart failure. *Am J Physiol Heart Circ Physiol* 2008;295:H2149-55.
- Bogaard HJ, Abe K, Vonk Noordegraaf A, Voelkel NF. The right

- ventricle under pressure: cellular and molecular mechanisms of right-heart failure in pulmonary hypertension. *Chest* 2009;135:794-804.
17. Borgdorff MA, Bartelds B, Dickinson MG, Steendijk P, Berger RM. A cornerstone of heart failure treatment is not effective in experimental right ventricular failure. *Int J Cardiol* 2013;169:183-9.
 18. Simon MA. Assessment and treatment of right ventricular failure. *Nat Rev Cardiol* 2013;10:204-18.
 19. Toischer K, Hartmann N, Wagner S, Fischer TH, Herting J, Danner BC, Sag CM, Hund TJ, Mohler PJ, Belardinelli L, Hasenfuss G, Maier LS, Sossalla S. Role of late sodium current as a potential arrhythmogenic mechanism in the progression of pressure-induced heart disease. *J Mol Cell Cardiol* 2013;61:111-22.
 20. Fang YH, Piao L, Hong Z, Toth PT, Marsboom G, Bache-Wiig P, Rehman J, Archer SL. Therapeutic inhibition of fatty acid oxidation in right ventricular hypertrophy: exploiting Randle's cycle. *J Mol Med (Berl)* 2012;90:31-43.
 21. Rocchetti M, Sala L, Rizzetto R, Staszewsky LI, Alemanni M, Zambelli V, Russo I, Barile L, Cornaghi L, Altomare C, Ronchi C, Mostacciolo G, Lucchetti J, Gobbi M, Latini R, Zaza A. Ranolazine prevents INaL enhancement and blunts myocardial remodelling in a model of pulmonary hypertension. *Cardiovasc Res* 2014;104:37-48.
 22. Lipke DW, Arcot SS, Gillespie MN, Olson JW. Temporal alterations in specific basement membrane components in lungs from monocrotaline-treated rats. *Am J Respir Cell Mol Biol* 1993;9:418-28.
 23. Lee JC, Cha CI, Kim DS, Choe SY. Therapeutic effects of umbilical cord blood derived mesenchymal stem cell-conditioned medium on pulmonary arterial hypertension in rats. *J Pathol Transl Med* 2015;49:472-80.
 24. McLaughlin VV, Gaine SP, Howard LS, Leuchte HH, Mathier MA, Mehta S, Palazzini M, Park MH, Tapson VF, Sitbon O. Treatment goals of pulmonary hypertension. *J Am Coll Cardiol* 2013;62(25 Suppl):D73-81.
 25. Sztrymf B, Souza R, Bertoletti L, Jaïs X, Sitbon O, Price LC, Simonneau G, Humbert M. Prognostic factors of acute heart failure in patients with pulmonary arterial hypertension. *Eur Respir J* 2010;35:1286-93.
 26. Vonk-Noordegraaf A, Haddad F, Chin KM, Forfia PR, Kawut SM, Lumens J, Naeije R, Newman J, Oudiz RJ, Provencher S, Torbicki A, Voelkel NF, Hassoun PM. Right heart adaptation to pulmonary arterial hypertension: physiology and pathobiology. *J Am Coll Cardiol* 2013;62(25 Suppl):D22-33.
 27. Bruneau BG, Piazza LA, de Bold AJ. BNP gene expression is specifically modulated by stretch and ET-1 in a new model of isolated rat atria. *Am J Physiol* 1997;273(6 Pt 2):H2678-86.
 28. Guihaire J, Bogaard HJ, Flécher E, Noly PE, Mercier O, Haddad F, Fadel E. Experimental models of right heart failure: a window for translational research in pulmonary hypertension. *Semin Respir Crit Care Med* 2013;34:689-99.
 29. Rajdev A, Garan H, Biviano A. Arrhythmias in pulmonary arterial hypertension. *Prog Cardiovasc Dis* 2012;55:180-6.
 30. Rich JD, Thenappan T, Freed B, Patel AR, Thisted RA, Childers R, Archer SL. QTc prolongation is associated with impaired right ventricular function and predicts mortality in pulmonary hypertension. *Int J Cardiol* 2013;167:669-76.
 31. Olsson KM, Nickel NP, Tongers J, Hoeper MM. Atrial flutter and fibrillation in patients with pulmonary hypertension. *Int J Cardiol* 2013;167:2300-5.
 32. Casserly B, Klinger JR. Brain natriuretic peptide in pulmonary arterial hypertension: biomarker and potential therapeutic agent. *Drug Des Devel Ther* 2009;3:269-87.
 33. Baliga RS, Zhao L, Madhani M, Lopez-Torondel B, Visintin C, Selwood D, Wilkins MR, MacAllister RJ, Hobbs AJ. Synergy between natriuretic peptides and phosphodiesterase 5 inhibitors ameliorates pulmonary arterial hypertension. *Am J Respir Crit Care Med* 2008;178:861-9.
 34. Schulz S, Singh S, Bellet RA, Singh G, Tubb DJ, Chin H, Garbers DL. The primary structure of a plasma membrane guanylate cyclase demonstrates diversity within this new receptor family. *Cell* 1989;58:1155-62.
 35. Hobbs AJ, Ignarro LJ. Nitric oxide-cyclic GMP signal transduction system. *Methods Enzymol* 1996;269:134-48.
 36. Schirger JA, Grantham JA, Kullo IJ, Jougasaki M, Wennberg PW, Chen HH, Lisy O, Miller V, Simari RD, Burnett JC Jr. Vascular actions of brain natriuretic peptide: modulation by atherosclerosis and neutral endopeptidase inhibition. *J Am Coll Cardiol* 2000;35:796-801.
 37. Liu SQ, Xie HW, Yan HY, Lu YQ, Wang LX. Recombinant B-type natriuretic peptide nesiritide attenuates vascular remodelling by reducing plasma aldosterone in rabbits. *Heart Lung Circ* 2012;21:551-5.
 38. Hsu JH, Yang SN, Chen HL, Tseng HI, Dai ZK, Wu JR. B-type natriuretic peptide predicts responses to indomethacin in premature neonates with patent ductus arteriosus. *J Pediatr* 2010;157:79-84.
 39. Shryock JC, Song Y, Rajamani S, Antzelevitch C, Belardinelli L. The arrhythmogenic consequences of increasing late INa in the cardiomyocyte. *Cardiovasc Res* 2013;99:600-11.
 40. Minotti G. Pharmacology at work for cardio-oncology: ranolazine to treat early cardiotoxicity induced by antitumor drugs. *J Pharmacol Exp Ther* 2013;346:343-9.